

# Excluding Stable Quark Matter: Insights from the QCD Vacuum Energy

Yang Bai<sup>a,b</sup> and Ting-Kuo Chen<sup>a</sup>

<sup>a</sup>*Department of Physics, University of Wisconsin-Madison, Madison, WI 53706, USA*

<sup>b</sup>*HEP Division, Argonne National Laboratory, Argonne, IL 60439, USA*

## Abstract

Quark matter (or quark nuggets), composed of quarks in the QCD deconfined and chiral-symmetry restored phase, has been conjectured to exist in nature for over half a century. With zero external pressure, it is stabilized by the balance between the quark Fermi pressure and the QCD vacuum pressure. Whether quark matter is more stable than ordinary nuclei has been a long-standing question, which requires understanding of the QCD vacuum energy. In this work, we employ both theoretical and data-driven methods to derive the QCD vacuum energy, utilizing the GMOR relation, the low-energy theorem, the equation of state from Lattice QCD, and the instanton gas/liquid model. The QCD vacuum energy is determined to be between  $(163 \text{ MeV})^4$  and  $(190 \text{ MeV})^4$ . Alongside the quark matter pressure calculated from perturbative QCD calculations, both the 2-flavor (via Bodmer) and 2+1-flavor (via Witten) quark matter are found to be more than 100 MeV per baryon heavier than the nucleons. Therefore, we exclude the possibility of quark matter being a more stable state than ordinary nuclei.

# Contents

- 1 Introduction** **2**
  
- 2 QCD vacuum energy** **3**
  - 2.1 From the GMOR relation . . . . . 4
  - 2.2 From the low-energy theorem . . . . . 5
  - 2.3 From the equation of state . . . . . 6
  - 2.4 From the instanton gas/liquid model . . . . . 10
  - 2.5 Summary: bounds on the QCD vacuum energy . . . . . 12
  
- 3 Quark matter stability** **12**
  
- 4 Discussion and conclusions** **16**
  
- A EQCD formulas for the quark-gluon plasma pressure** **18**
  
- B Bag parameter inference in the hot  $SU(3)$  theory** **20**

# 1 Introduction

Long ago proposed by physicists such as Bodmer [1], Lee and collaborators [2–5], and Witten [6], quark nuggets, the solitonic “bags” of quark matter (*i.e.*, deconfined quarks) existing in the zero-pressure vacuum, might in fact be the global ground state of baryon matter in quantum chromodynamics (QCD) instead of ordinary hadron matter. The study of their possible existence is not only of theoretical importance to the exploration of QCD, but can also potentially lead to various phenomenological consequences. For instance, they could extend the periodic table by introducing “exotic nuclei” with very large atomic and atomic mass numbers [7]. Furthermore, if they were produced in the early universe and remain stable at the present time, they could serve as a compelling dark matter candidate [6]. As a result, one of the most crucial questions about quark matter is its stability, which, intriguingly, has remained unanswered for half a century until now.

Quark matter is stabilized by the balance between the quark matter pressure described by perturbative QCD (pQCD) and the nonperturbative QCD vacuum pressure, often collectively described by the so-called “bag parameter”. The latter of these is closely tied to the QCD trace anomaly that consists of two major parts: the gluon condensate that determines confinement and the quark bilinear condensates that determine chiral symmetry. While, as we will discuss later, one could in principle consider some more complicated scenarios that involve partial symmetry restorations, we will assume complete deconfinement with zero gluon condensate and chiral-symmetry restoration with zero quark bilinear condensates inside the quark nugget bags, the same as in Ref. [6]. For a given balanced quark matter system, one can infer the associated energy per baryon  $\epsilon/n_B$ . If  $\epsilon/n_B \leq 930$  MeV, the averaged mass per nucleon of the iron element (the most stable nucleus), then the quark matter is stable in the thermodynamic limit (it will become less stable once finite-size effects are included) and vice versa. To pin down the value of  $\epsilon/n_B$ , it is essential to study pQCD and the QCD vacuum energy with sufficient precision.

On the pQCD side, the calculation of quark matter equation of state at finite baryon chemical potential has been carried out up to  $\mathcal{O}(g^4)$  in Ref. [8] and more recently completed up to  $\mathcal{O}(g^6)$  in Ref. [9]. Here,  $g$  is the QCD gauge coupling. As for the finite-temperature direction, the framework of electrostatic QCD (EQCD) [10, 11] has been established up to  $\mathcal{O}(g^6)$  [12] for massless quarks, while the massive quark effects have been accounted for up to  $\mathcal{O}(g^2)$  [13], with the caveat of the still unknown nonperturbative contribution at  $\mathcal{O}(g^6)$  [14, 15] which we will discuss more later. Moreover, when the quark number density is high enough, a considerable superconducting gap will be induced, which will then lead to the formation of quark Cooper pairs and thus the phenomenon of color superconductivity. In principle, the associated energy gap will also contribute to the quark matter pressure, but, as shown in Refs. [16, 17] and analyzed in Ref. [18], the corresponding contribution of  $qq$  Cooper pairs to the baryon matter pressure is negligible for our purpose of studying quark matter stability.

On the other hand, because of its nonperturbative nature, determining the QCD vacuum energy (or bag parameter) is the most challenging part of the question of quark matter stability. To approach this issue, we analyze it from the following four perspectives:

1. The Gell-Mann, Oakes, Renner (GMOR) relation [19], which establishes a direct connection between the quark condensates and the pion mass and decay constant (also noticed in Ref. [20]).

2. The low-energy theorem for QCD [21] and the measurement of QCD topological susceptibility  $\chi_t$  through lattice QCD (LQCD) [22], which provides a robust lower bound on the gluonic contribution to the bag parameter.
3. The fitting to the isospin-dense LQCD (LQCD<sub>I</sub>) [23] and finite-temperature LQCD (LQCD<sub>T</sub>) [24–26] equations of state based on the frameworks of pQCD and EQCD, respectively.<sup>1</sup> The former has already been conducted in Ref. [18], while the latter is presented in this study. Although the currently available calculations still cannot resolve the value of QCD vacuum energy due to data uncertainties, they can provide reliable upper bounds on it.
4. The instanton gas/liquid model, which provides a fairly accurate prediction for the vacuum energy of the pure  $SU(3)$  Yang-Mills theory. Though in real QCD dynamical quarks play a major role and thus somewhat spoil the dilute instanton picture, we still present our analysis in this study and provide the corresponding (unreliable) prediction for the gluonic QCD vacuum energy.

As we will eventually show, it is sufficient to exclude both stable 2- and 2+1-flavor quark matter using methods 1 and 2 above, which is the main conclusion of our study that finally settles the long-standing quest for stable quark matter. Compared to a recent study in Ref. [31] using a phenomenological linear sigma model, we have included the important gluonic contribution to the QCD vacuum energy that is neglected in Ref. [31] and arrived at an opposite conclusion about the stability of the 2-flavor quark matter.

Our paper is organized as follows. In Section 2, we define the QCD vacuum energy in terms of the QCD trace anomaly and investigate it from the four perspectives mentioned above, with the details of the EQCD formulas presented in Appendix A and those of the hot  $SU(3)$  LQCD fit in Appendix B. After that, we discuss the issue of quark matter stability using the previously obtained results and exclude the existence of both stable 2- and 2+1-flavor quark matter in Section 3. Finally, we discuss and conclude our study in Section 4.

## 2 QCD vacuum energy

In the physical QCD vacuum with zero chemical potential and temperature, the QCD vacuum energy is usually related to the quark-anti-quark (or simply quark) and gluon condensates. The former is associated with the breaking of chiral symmetry, while the latter is not associated with any apparent symmetry in real QCD with quarks.<sup>2</sup> More explicitly, the QCD vacuum energy is related to the trace anomaly of QCD which results from the breaking of the classical dilatation

---

<sup>1</sup>We have also considered the matching between the LQCD calculations of trace anomaly contributions to nuclear masses (see for example Refs. [27, 28]) and the associated low-density theorems for nucleons and pions in Ref. [29] and Ref. [30], respectively. However, as LQCD only measures the differential contributions between the physical vacuum and the nuclear state, it is impossible to extract the warranted QCD vacuum energy with this approach.

<sup>2</sup>In the pure  $SU(N_c)$  Yang-Mills theories, the Polyakov loop associated with the  $Z_{N_c}$  center symmetry serves as a good gauge-invariant order parameter to describe confinement [32]. After including quarks in the fundamental representation as in real QCD, this center symmetry is no longer intact.

symmetry at the quantum level. This trace anomaly operator is given by

$$\Theta_\mu^\mu \equiv \left[ \frac{\beta(g)}{2g} G_a^{\mu\nu} G_{\mu\nu}^a + \sum_{q=u,d,s} m_q \gamma_m(g) \bar{q}q \right] + \left[ \sum_{q=u,d,s} m_q \bar{q}q \right]. \quad (2.1)$$

Here,  $\Theta_\mu^\mu$  is the trace anomaly operator that depends on the renormalized fields and the QCD gauge coupling  $g$  [33, 34],  $\beta(g)$  is the beta-function of the gauge coupling, and  $\gamma_m(g)$  is the quark mass anomalous dimension [35]. Note that the quantities inside each bracket are altogether renormalization-scale invariant.

Usually, one defines the QCD vacuum energy as  $-\frac{1}{4}$  times the vacuum expectation value (VEV) of the trace anomaly in the physical vacuum, or  $-\frac{1}{4}\langle\Theta_\mu^\mu\rangle_0$ . For the convenience of QCD at high temperature or density, one can make a more general definition of the QCD vacuum energy as the nonperturbative (NP) contributions to the trace anomaly, being separated from the perturbative contributions. We use  $B(\mu, T)$  to denote the QCD ‘‘vacuum’’ energy in a matter state with chemical potential  $\mu$  and temperature  $T$  and define it as

$$B(\mu, T) \equiv \frac{1}{4} [\langle\Theta_\mu^\mu\rangle_{\text{NP}}(\mu, T) - \langle\Theta_\mu^\mu\rangle_0]. \quad (2.2)$$

The usual QCD vacuum energy is quoted to be  $\mu$ - and  $T$ -independent, as given by

$$B^{\text{con}} \equiv B(\mu \rightarrow \infty, T) = B(\mu, T \rightarrow \infty) = -\frac{1}{4}\langle\Theta_\mu^\mu\rangle_0, \quad (2.3)$$

*i.e.*, at either high temperature or high chemical potential, the corresponding QCD quark-gluon plasma phase is fully deconfined with the chiral symmetry fully restored, and thus  $\langle\Theta_\mu^\mu\rangle_{\text{NP}} = 0$  (the potential color superconducting phase in dense matter will be discussed later).

The main goal of this section is to obtain  $B^{\text{con}}$ , which contains two renormalization-scale invariant parts,

$$B_G^{\text{con}} = -\frac{1}{4}\left\langle\frac{\beta(g)}{2g}G_a^{\mu\nu}G_{\mu\nu}^a + \sum_q m_q \gamma_m(g) \bar{q}q\right\rangle_0, \text{ and} \quad (2.4)$$

$$B_F^{\text{con}} = -\frac{1}{4}\left\langle\sum_q m_q \bar{q}q\right\rangle_0. \quad (2.5)$$

In the following, we will utilize several theoretical approaches, with or without Lattice QCD (LQCD) inputs, to obtain either partial or complete information (lower or upper bounds) of  $B_G^{\text{con}}$  and/or  $B_F^{\text{con}}$ . These approaches are ordered based on their rigor and the confidence we have in their produced results, which is, of course, subject to our own understanding.

## 2.1 From the GMOR relation

We begin our discussion of the QCD vacuum energy using the Gell-Mann, Oakes, Renner (GMOR) relation [19], which was mentioned in Ref. [20] and presented in Ref. [18]. Here, we simply summarize the results. For the  $u, d$  light quarks, one has

$$\frac{f_\pi^2 m_\pi^2}{2} = -m_\ell \langle\bar{\ell}\ell\rangle, \quad \ell = u, d, \quad (2.6)$$

where  $f_\pi \approx 92$  MeV is the pion decay constant,  $m_\pi \approx 135$  MeV is the pion mass, and  $m_\ell = (m_u + m_d)/2$  is the averaged light quark mass. Using the  $\overline{\text{MS}}$  scheme at 2 GeV, one gets that  $\langle \bar{\ell}\ell \rangle^{\overline{\text{MS}}}(2 \text{ GeV}) = -(272 \text{ MeV})^3$  based on the  $SU(2)$  chiral perturbation theory [36], as well as  $m_u = 2.16$  MeV,  $m_d = 4.70$  MeV, and  $m_s = 93.5$  MeV [37], and thus

$$B_{F,2}^{\text{con}} = -\frac{1}{4} \sum_{q=u,d} \langle m_q \bar{q}q \rangle^{\overline{\text{MS}}}(2 \text{ GeV}) = (76.8 \text{ MeV})^4 . \quad (2.7)$$

Correspondingly, the  $s$ -quark condensate  $\langle \bar{s}s \rangle$  is further given by lattice measurement [38] and sum rule average [39] respectively by [18]

$$\frac{\langle \bar{s}s \rangle^{\overline{\text{MS}}}(2 \text{ GeV})}{\langle \bar{\ell}\ell \rangle^{\overline{\text{MS}}}(2 \text{ GeV})} = \begin{cases} 1.08 \pm 0.16 & \text{[Lattice]} \\ 0.66 \pm 0.10 & \text{[Sum Rule Average]} \end{cases} , \quad (2.8)$$

which leads to

$$B_{F,2+1}^{\text{con}} \equiv -\frac{1}{4} \sum_{q=u,d,s} \langle m_q \bar{q}q \rangle^{\overline{\text{MS}}}(2 \text{ GeV}) = \begin{cases} (153^{+6.0}_{-6.0} \text{ MeV})^4 & \text{[Lattice]} \\ (136 \pm 5.0 \text{ MeV})^4 & \text{[Sum Rule Average]} \end{cases} . \quad (2.9)$$

For later convenience, we will label the above values as  $\text{GMOR}_L$  and  $\text{GMOR}_S$ , respectively.

## 2.2 From the low-energy theorem

In this subsection, we combine the NSVZ low-energy theorem (LET) and the LQCD calculation of topological susceptibility to derive a lower bound on  $B_G^{\text{con}}$ . The NSVZ LET can be derived using the anomalous Ward identity of the dilatation symmetry [21], which states that

$$\lim_{q \rightarrow 0} i \int d^4x e^{iqx} \langle T \mathcal{O}(x) \Theta_\mu^\mu(0) \rangle_0 = (-d_\mathcal{O}) \langle \mathcal{O} \rangle_0 . \quad (2.10)$$

Here,  $T$  stands for time ordering and  $d_\mathcal{O}$  is the engineer dimension of the operator  $\mathcal{O}$ , with  $d_\mathcal{O} = 4$  for  $\mathcal{O} = G_a^{\mu\nu} G_a^{\mu\nu}$  and  $d_\mathcal{O} = 3$  for  $\mathcal{O} = \bar{q}q$ . To the leading order in small quark mass and using the one-loop beta function for the gauge coupling, one has

$$\lim_{q \rightarrow 0} i \int d^4x e^{iqx} \left\langle T \mathcal{O}(x) \frac{\alpha_s}{8\pi} G^2(0) \right\rangle_0 = \frac{d_\mathcal{O}}{\beta_0} \langle \mathcal{O} \rangle_0 + O(m_q) , \quad (2.11)$$

where we have suppressed the Lorentz indices of the field strength tensors and simply write  $G_{\mu\nu}^a G_a^{\mu\nu} \equiv G^2$ . Here,  $\beta_0 = (11N_c - 2N_f)/3$  is the coefficient of the leading term in  $\beta(\alpha_s) \equiv d\alpha_s/d \log \mu = -\beta_0 \alpha_s^2/(2\pi) + O(\alpha_s^3)$  [note that  $\beta(g) \equiv dg/d \log \mu = -\beta_0 g^3/(16\pi^2) + O(g^5)$ ]. For our purpose of estimating the gluonic contribution to the QCD vacuum energy, we ignore the  $O(m_q)$  corrections and make a more conservative estimation.

Applying the LET to the  $G^2$  operator with  $d_\mathcal{O} = 4$ , one has

$$i \int d^4x \left\langle T \frac{\alpha_s}{8\pi} G^2(x) \frac{\alpha_s}{8\pi} G^2(0) \right\rangle_0 = \frac{4}{\beta_0} \left\langle \frac{\alpha_s}{8\pi} G^2 \right\rangle_0 , \quad (2.12)$$

where we have used the equal sign by ignoring the small quark mass corrections. In the following, we will show that the left-hand side of the above equation can be related to the topological susceptibility through a simple algebraic inequality. We first translate this equation from the Minkowski spacetime to the Euclidean spacetime (note that  $\tau = it$ ,  $G^2 = -G_E^2$  and  $G\tilde{G} = iG_E\tilde{G}_E$  with  $\tilde{G} \equiv \tilde{G}^{\mu\nu} = \frac{1}{2}\epsilon^{\mu\nu\rho\sigma}G_{\rho\sigma}$ , where the fields without subscripts are defined in the Minkowski spacetime). Using the inequality

$$G_E^2 = \frac{1}{2}(G_E^2 + \tilde{G}_E^2) = \frac{1}{2} \left[ (G_E - \tilde{G}_E)^2 + 2G_E\tilde{G}_E \right] \geq G_E\tilde{G}_E, \quad (2.13)$$

one can show that

$$\begin{aligned} \frac{4}{\beta_0} \left\langle \frac{\alpha_s}{8\pi} G^2 \right\rangle_0 &= \int d^4x_E \left\langle T \frac{\alpha_s}{8\pi} G_E^2(x) \frac{\alpha_s}{8\pi} G_E^2(0) \right\rangle_0 \\ &\geq \int d^4x_E \left\langle T \frac{\alpha_s}{8\pi} G_E\tilde{G}_E(x) \frac{\alpha_s}{8\pi} G_E\tilde{G}_E(0) \right\rangle_0 \equiv \chi_t \end{aligned} \quad (2.14)$$

$$\Rightarrow B_G^{\text{con}} \geq \frac{\beta_0^2}{16} \chi_t. \quad (2.15)$$

In the last step, we ignored the positive  $\gamma_m$ -term in  $B_G^{\text{cons}}$ , thus making the above lower bound more conservative.<sup>3</sup>

The topological susceptibility,  $\chi_t$ , is a measure of the fluctuation of the topological charge  $Q(x) = \frac{g^2}{32\pi^2} G_E\tilde{G}_E(x)$  throughout spacetime. In the Euclidean spacetime, one simply has  $\chi_t = \langle Q^2 \rangle / V$  with  $V$  as the spacetime 4-volume. Based on chiral perturbation theory, one can relate  $\chi_t$  to the pion mass and decay constant as  $\chi_t = \frac{1}{4}(1 + O[m_\pi^2/(4\pi f_\pi)^2])m_\pi^2 f_\pi^2$  [41–44]. Refs. [22, 45] have used LQCD to perform precise calculations of this quantity and reported results that are consistent with the prediction of the chiral perturbation theory. Here, we take the zero-temperature value in Ref. [22],  $\chi_t = (75.6 \pm 2.0 \text{ MeV})^4$ , after combining the statistical and systematic errors.

Substituting the value of  $\chi_t$  into the bound given in Eq. (2.15) and taking  $\beta_0 = 9$  with  $N_c = 3$  and  $N_f = 3$ , we arrive at a robust lower bound for  $B_G^{\text{con}}$ ,

$$B_G^{\text{con}} \geq \frac{\beta_0^2}{16} \chi_t = (113.4 \text{ MeV})^4. \quad (2.16)$$

### 2.3 From the equation of state

The third way we infer about the QCD vacuum energy is by analyzing the equation of state calculated through LQCD at either finite temperature (LQCD<sub>T</sub>) or finite isospin density (LQCD<sub>I</sub>). We first recap our previous analysis of the LQCD<sub>I</sub> data based on the perturbative QCD (pQCD) framework [18]. By comparing the combined predictions of pQCD at finite density [8] and the color superconducting (CS) gap [16, 17] to the LQCD<sub>I</sub> data from Ref. [23] (earlier results can be found in Ref. [46]), we obtained the 90% CL upper bound on  $B_2^{\text{con}}$  as

$$B_2^{\text{con}} \lesssim (160 \text{ MeV})^4, \quad (\text{from LQCD}_I). \quad (2.17)$$

---

<sup>3</sup>Keeping the leading term in  $\mathcal{O}(m_q)$ , the bound becomes  $B_G - \frac{1}{4}\langle\gamma_m m_q \bar{q}q\rangle \geq \frac{\beta_0^2}{16}\chi_t - \frac{3}{16}\langle m_q \bar{q}q\rangle$ , where  $\gamma_m \equiv -d \ln m_R(\mu)/d \ln \mu = 2\alpha_s/\pi + \mathcal{O}(\alpha_s^2)$  with  $m_R(\mu)$  as the renormalized quark mass [35, 40]. Note that since  $\langle m_q \bar{q}q\rangle < 0$  and that  $\gamma_m < 3/4$  for a perturbative  $\alpha_s$ , the bound becomes more stringent after including the leading term in  $\mathcal{O}(m_q)$ .

As we will discuss more later, it is plausible that the  $s$ -quark condensate remains nonzero and intact in the isospin-dense system. If we naively add the  $s$ -quark contribution from Eq. (2.8) to this upper bound, we obtain the upper limit on the total QCD vacuum energy

$$B_{2+1}^{\text{con}} \lesssim \begin{cases} (185 \text{ MeV})^4 & \text{[Lattice]} \\ (176 \text{ MeV})^4 & \text{[Sum Rule Average]} \end{cases}, \quad (\text{from LQCD}_I). \quad (2.18)$$

We can also subtract the light-flavor contributions to obtain an upper bound on  $B_G^{\text{con}}$  as

$$B_G^{\text{con}} \lesssim (158 \text{ MeV})^4, \quad (\text{from LQCD}_I). \quad (2.19)$$

However, it is worth noting that  $B$  can in principle be  $\mu_I$ -dependent, as we discussed in Section 2, though we do not know at this point the proper way to model this dependence. This is also the case for our discussion of the hot QCD system, as we now address.

To model the thermodynamic properties of a zero-density hot QCD system, we refer to the framework of electrostatic QCD (EQCD), which is an effective field theory formulated by integrating out the “hard modes” with energies of  $\mathcal{O}(2\pi T)$  and above after performing dimensional reduction [10, 11]. The corresponding grand potential has been studied in the massless quark limit at orders  $\mathcal{O}(g^2)$  [47, 48],  $\mathcal{O}(g^3)$  [49],  $\mathcal{O}(g^4 \ln(1/g))$  [50],  $\mathcal{O}(g^4)$  [51, 52],  $\mathcal{O}(g^5)$  [53], and  $\mathcal{O}(g^6 \ln(1/g))$  [12], while the massive quark effects have been studied up to  $\mathcal{O}(g^2)$  [13]. It is long known that nonperturbative effects kick in at  $\mathcal{O}(g^6)$ , which result from the infinite number of diagrams contributing to the grand potential through the gluon magnetic mass at the same order [14, 15]. Although some of these nonperturbative terms have been studied in the literature [54, 55], including the most recent Ref. [56], the full expression at  $\mathcal{O}(g^6)$  remains unknown. To address this issue, we follow the common prescription of assigning a dimensionless parameter  $\Delta$  at  $\mathcal{O}(g^6)$  to be fitted from the lattice data, assuming that it can successfully describe the nonperturbative effects.<sup>4</sup> As we will show later, this prescription can describe the lattice data very efficiently, though one cannot know at this point the correctness of the parameter choice. The quantity that we choose to fit is the normalized trace anomaly,

$$\frac{\Theta^\mu{}_\mu}{T^4} = T \frac{\partial}{\partial T} \left( \frac{p_{\text{QCD}}}{T^4} \right) = T \frac{\partial}{\partial T} \left( \frac{p_{\text{QCD,m}}}{T^4} \right) + \frac{4B_{2+1}^{\text{con}}}{T^4}, \quad (2.20)$$

where the EQCD formulas for the total QCD pressure  $p_{\text{QCD}}$  and the quark-gluon plasma pressure  $p_{\text{QCD,m}}$  are summarized in Appendix A. Note that here  $\Theta^\mu{}_\mu$  stands for the VEV of the trace anomaly operator in the finite-temperature vacuum in accordance with the LQCD notation and should not be confused with the operator defined earlier in Section 2. Here, we have chosen to model the QCD vacuum energy using the constant value  $B_{2+1}^{\text{con}}$ , which is only asymptotically valid at high enough  $T$  given the crossover nature of the QCD phase transition in the normal QCD vacuum [57, 58]. Otherwise, one might need to consider additional temperature-dependent bag parameters, which do not directly contribute to the zero-temperature quark matter properties but may affect the fit to the LQCD data. Note that after fixing the number of flavors  $N_f = 2+1$ , one has  $p_{\text{QCD,m}} = p_{\text{QCD,m}}(X_T, T)$ , where  $X_T \equiv \bar{\mu}/(2\pi T)$  is the renormalization scale parameter

---

<sup>4</sup>The argument for the validity of this prescription can be found in Ref. [12], which relies on the  $T$ - and  $\bar{\mu}$ -dependence of the unknown  $\mathcal{O}(g^6)$  terms.



with  $\bar{\mu}$  being the renormalization scale of the system. The reason for this parametrization, as we have argued in Ref. [18], is because of the uncertainty in the choice of  $\bar{\mu}$  with respect to the actual physical scale of a given system (see Refs. [8, 59] for example). As a result, there are three parameters to fit from the LQCD<sub>T</sub> data:  $X_T$ ,  $\Delta$ , and  $B_{2+1}^{\text{con}}$ . Since one should expect the confined plus chiral-symmetry-broken phase to have a lower vacuum energy than the deconfined and chiral-symmetry-restored phase, we require a priori that  $B_{2+1}^{\text{con}} \geq 0$ .

On the other hand, the LQCD calculations of the zero-density 2+1-flavor hot QCD system had been carried out up to  $T \sim 400$  MeV by the Wuppertal-Budapest (WB) collaboration [24] and  $\sim 500$  MeV by the HotQCD collaboration [25]. Later on, Ref. [26] (BPW) pushed the calculation further up to  $T \sim 2$  GeV. More recently, Ref. [60] has performed the simulations for  $N_f = 3$  massless quarks and  $T \sim 3\text{--}165$  GeV. Since the bag parameter is only relevant in the low- $T$  regime, we do not include this latest dataset in our current study. In principle, one should expect the EQCD and LQCD<sub>T</sub> calculations to match only when  $T$  is considerably high where one can trust the perturbative calculations. Therefore, we truncate the data by introducing a starting temperature  $T_{\text{start}}$  and only fit the data with  $T \geq T_{\text{start}}$ . Nevertheless, as we will demonstrate below, the  $\Delta$  prescription renders a pretty good fit even down to  $T_{\text{start}} = 300$  MeV. We collect the trace anomaly data measured in these works in Figure 1, where the errorbars contain both systematic and statistical uncertainties.

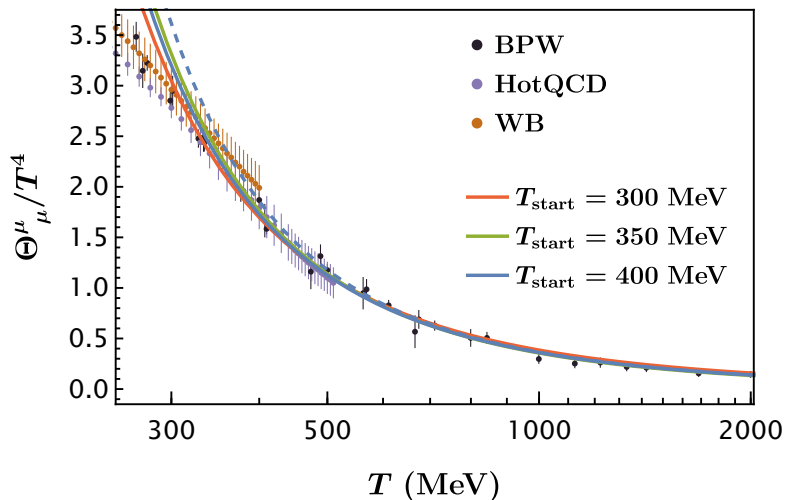


Figure 1: The lattice trace anomaly data of the zero-density 2+1-flavor hot QCD (LQCD<sub>T</sub>) system from Refs. [24–26], as well as the best-fit curves (solid) with  $T_{\text{start}} = 300, 350, 400$  MeV. For illustration purposes, we also show the dashed line which is for the  $T_{\text{start}} = 400$  MeV best-fit point but with a nonzero  $B_{2+1}^{\text{con}} = (170 \text{ MeV})^4$ . Note that the errorbars of the LQCD<sub>T</sub> data contain both systematic and statistical uncertainties.

We choose  $T_{\text{start}} = 300, 350, 400$  MeV, and the best-fit points as well as the corresponding degrees of freedom  $k$  and  $\chi^2$  values are given by

$$\begin{aligned}
 T_{\text{start}} = 300 \text{ MeV} : & \quad (k, \chi^2, X_T, \Delta, B_{2+1}^{\text{con}}) = (71, 55.8, 1.65, -3338, 0) , \\
 T_{\text{start}} = 350 \text{ MeV} : & \quad (k, \chi^2, X_T, \Delta, B_{2+1}^{\text{con}}) = (52, 23.6, 1.52, -3087, 0) , \\
 T_{\text{start}} = 400 \text{ MeV} : & \quad (k, \chi^2, X_T, \Delta, B_{2+1}^{\text{con}}) = (35, 13.2, 1.56, -3155, 0) ,
 \end{aligned}
 \tag{2.21}$$

with the corresponding best-fit curves shown in Figure 1. One can see that all the curves describe the LQCD<sub>T</sub> data very well, even in the high- $T$  regime where the uncertainties are relatively small. On the other hand, because of the large uncertainties in the low- $T$  regime where  $B_{2+1}^{\text{con}}$  plays a more significant role, the value of  $B_{2+1}^{\text{con}}$  remains unresolvable with the current LQCD<sub>T</sub> measurements. For comparison, we also show the curve predicted by the  $T_{\text{start}} = 400$  MeV best-fit point but with  $B_{2+1}^{\text{con}} = (170 \text{ MeV})^4$ , which still agrees well with the high- $T$  data but clearly deviates from the low- $T$  data more compared to the original best-fit curve. Moreover, the parameter  $\Delta$  adds another layer of complication to the problem as it might falsely capture some of the effects that should be attributed to  $B_{2+1}^{\text{con}}$ . We also note that the data could prefer  $B_{2+1}^{\text{con}} < 0$ , which we do not take into account since it is unphysical as stated before.

To obtain the constraints on the model parameters, we present the two-parameter 90% confidence level (CL) contours on the  $[X_T, (B_{2+1}^{\text{con}})^{1/4}]$  and  $[\Delta, (B_{2+1}^{\text{con}})^{1/4}]$  planes in Figure 2. We also show the lower bounds on  $B_{2+1}^{\text{con}}$  based on the values of the quark condensates derived from the GMOR relation (see Section 2.1) and the low-energy theorem (LET) (see Section 2.2) in Figure 2. In both parameter spaces, the upper bounds inferred from the  $T_{\text{start}} = 300$  MeV case are in tension with the lower bounds derived before, while for the  $T_{\text{start}} = 350$  and 400 MeV cases, the loosest bound  $B_{2+1}^{\text{con}} \lesssim (190 \text{ MeV})^4$  shows up when we fix the best-fit  $\Delta$  for  $T_{\text{start}} = 400$  MeV. Consequently, we arrive at the following upper bound on the QCD vacuum energy based on the 2+1-flavor hot QCD system

$$B_{2+1}^{\text{con}} \lesssim (190 \text{ MeV})^4, \quad (\text{from LQCD}_T), \quad (2.22)$$

which is consistent with the bounds obtained from the pQCD+LQCD<sub>I</sub>+CS analysis if we assume that the  $s$ -quark condensate remains nonzero and intact in the isospin-dense system.

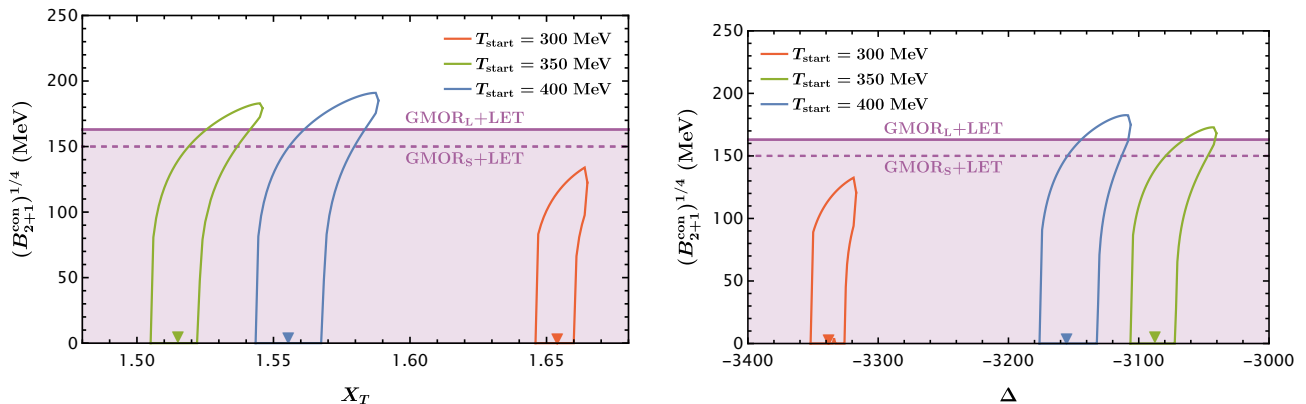


Figure 2: *Left panel:* The two-parameter 90% CL contours on the  $[X_T, (B_{2+1}^{\text{con}})^{1/4}]$  plane for  $T_{\text{start}} = 300, 350, 400$  MeV. The horizontal lines are the lower bounds on  $B_{2+1}^{\text{con}}$  derived from the GMOR relation using either the lattice (GMOR<sub>L</sub>) or the sum rule average (GMOR<sub>S</sub>) [see Eq. (2.9)] plus the low-energy theorem (LET) [see Eq. (2.16)]. *Right panel:* Same as the left panel but on the  $[\Delta, (B_{2+1}^{\text{con}})^{1/4}]$  plane.

Subtracting the  $s$ -quark condensate contribution from the total vacuum energy, one obtains

the upper bound on  $B_2^{\text{con}}$  for the two light flavor system as

$$B_2^{\text{con}} \lesssim \begin{cases} (168 \text{ MeV})^4 & \text{[Lattice]} \\ (178 \text{ MeV})^4 & \text{[Sum Rule Average]} \end{cases}, \quad (\text{from LQCD}_T). \quad (2.23)$$

Further subtracting the light-quark condensate contributions, one then has the upper bound on  $B_G^{\text{con}}$  as

$$B_G^{\text{con}} \lesssim \begin{cases} (166 \text{ MeV})^4 & \text{[Lattice]} \\ (176 \text{ MeV})^4 & \text{[Sum Rule Average]} \end{cases}, \quad (\text{from LQCD}_T). \quad (2.24)$$

For the following study on quark matter stability, we will only use the upper bound derived from LQCD<sub>I</sub> for  $B_2^{\text{con}}$  and that from LQCD<sub>T</sub> for  $B_{2+1}^{\text{con}}$  so as to match the LQCD simulation setups with the corresponding directly inferred upper bounds:

$$B_2^{\text{con}} \lesssim (160 \text{ MeV})^4, \quad B_{2+1}^{\text{con}} \lesssim (190 \text{ MeV})^4. \quad (2.25)$$

## 2.4 From the instanton gas/liquid model

The last way we investigate the QCD vacuum energy is based on the instanton gas/liquid model. To fully appreciate this perspective, we need to first discuss the pure Yang-Mills theory. In addition to the LQCD data, we also perform an EQCD fit to the thermal  $SU(3)$  lattice data from Refs. [61, 62] by setting  $N_f = 0$ . We leave the details of the fit to Appendix B and only summarize the results here. Compared to the LQCD<sub>T</sub> data, the lattice simulations of the  $SU(N_c)$  theories yield much smaller uncertainties and thus allow us to actually extract the constant bag parameter  $B_{\text{YM}}^{\text{con}} \equiv B_{\text{YM}}$ , which, for various choices of  $T_{\text{start}}$ , is consistently given by  $B_{\text{YM}} \sim (250 \text{ MeV})^4$  for  $N_c = 3$ .

As already pointed out in Ref. [63], this result can actually be well described by the dilute instanton gas model. To see this, we analyze the topological susceptibility  $\chi_t = \langle Q^2 \rangle / V$  of the system [see Eq. (2.14) for its definition]. Suppose the instanton gas is dilute enough for us to neglect the correlations between the instanton and anti-instanton distributions, we can then use Poisson statistics and the random-walk theory in 4 dimensions to obtain

$$\sqrt{\langle Q^2 \rangle} = \frac{3}{4} \sqrt{\frac{\pi}{2}} \sqrt{N} = \frac{3}{4} \sqrt{\frac{\pi}{2}} \sqrt{N_I + N_A} \approx 0.93 \sqrt{n_I V}, \quad (2.26)$$

where  $N_{I,A}$  are the numbers of instantons and anti-instantons and  $n_I$  denotes the effective instanton density in 4-dimensional spacetime. As a result, we can derive [64]

$$B_{\text{YM}} = -\frac{1}{4} \left\langle \frac{\beta(g)}{2g} G^2 \right\rangle_0 \approx \frac{1}{4} \frac{11N_c}{3} n_I = \frac{11N_c}{12} \frac{\chi_t}{0.93^2}. \quad (2.27)$$

Using the lattice data from Ref. [65] with  $\chi_t^{1/4} = 176.8(2.7)(4.2) \text{ MeV}$ , we obtain  $B_{\text{YM}} \approx (236 \text{ MeV})^4$ , which is indeed in agreement with our direct EQCD fit. This suggests that in the absence of quarks, the dilute instanton gas model is a decent model for studying the thermodynamic properties of the gluon fields. This is also supported by the following fact: we can

calculate the average distance among individual instantons as  $R = [n_{\text{I}}(\pi^2/2)]^{-1/4} \approx 0.72$  fm. Then, we quote the instanton number density distribution function [66]

$$n_{\text{I}}(\rho_{\text{max}}) = \int_0^{\rho_{\text{max}}} d\rho \frac{0.47 e^{-1.68 N_c}}{(N_c - 1)!(N_c - 2)!} \left( \frac{8\pi^2}{g^2(\rho)} \right)^{2N_c} e^{-8\pi^2/g^2(\rho)} \rho^{-5}, \quad (2.28)$$

where  $\rho$  is the instanton size and  $\rho_{\text{max}}$  is the size cutoff. Using  $n_{\text{I}} = \chi_t/0.93^2$ , one has  $\rho_{\text{max}} \approx 0.25$  fm for the reference scale  $\Lambda_{\overline{\text{MS}}} \approx 1.26 T_c \approx 340$  MeV [61]. The small ratio  $\rho_{\text{max}}/R$  thus justifies the dilute instanton gas approximation (see Ref. [64] for emphasizing this point).

Once dynamical quarks are included in the theory (such as real-world QCD), it is no longer straightforward to apply the dilute instanton gas picture. 't Hooft has shown that the presence of light quarks will suppress the instanton density by  $\sim (m_q)^{N_f}$  [66], although spontaneous chiral symmetry breaking could generate a dynamical quark mass to overtake the small current quark mass effects [67, 68]. As a result, the simple relation between  $\chi_t$  and  $n_{\text{I}}$  given in Eq. (2.26) is no longer supported (this is also hinted at by the instanton number density distribution given by the lattice study in Ref. [69]).

Nevertheless, it is still worth exploring ways to improve the instanton gas model, such as the effective bosonic theory based on the spectrum of pseudoscalar mesons that incorporates the screening effects on the instanton density presented in Ref. [70]. Since instantons are related to both the spontaneous breaking of the chiral symmetry and the  $U(1)_A$  anomaly, one can write down the following mass matrix of the  $(\eta_0, \eta_8)$  generator fields to the leading order in quark mass,

$$V = \frac{1}{2} \left( \frac{4}{3} m_K^2 - \frac{1}{3} m_\pi^2 \right) \eta_8^2 + \frac{1}{2} \left( \frac{2}{3} m_K^2 + \frac{1}{3} m_\pi^2 \right) \eta_0^2 + \frac{1}{2} \frac{4\sqrt{2}}{3} (m_\pi^2 - m_K^2) \eta_8^2 + \frac{N_f}{f_\pi^2} n_{\text{I}} \eta_0^2, \quad (2.29)$$

where  $n_{\text{I}}$  is related to the meson masses through the Witten-Veneziano relation [71, 72],

$$f_\pi^2 (m_{\eta'}^2 + m_\eta^2 - 2m_K^2) = 2N_f n_{\text{I}}. \quad (2.30)$$

Once the mesonic degrees of freedom are taken into consideration, one can then use the phenomenon of topological charge screening to derive the correction to the topological susceptibility,

$$\chi_t = n_{\text{I}} - \frac{2N_f}{f_\pi^2} n_{\text{I}}^2 \int d^4x [\cos^2(\phi) D(m_{\eta'}, x) + \sin^2(\phi) D(m_\eta, x)], \quad (2.31)$$

where  $\phi$  is the  $\eta - \eta'$  mixing angle and  $D(m, x) = m/(4\pi^2 x) K_1(mx)$  is the Euclidean propagator of a scalar particle with  $K_1$  as the modified Bessel function of the second kind. After plugging in the physical masses and diagonalizing Eq. (2.29), one has

$$\chi_t \approx 0.05 n_{\text{I}} \quad \Rightarrow \quad B_G^{\text{con}} \approx \frac{\beta_0}{4} \times 20 \chi_t = (196 \text{ MeV})^4, \quad (2.32)$$

where we have again used the lattice result in Ref. [22] with  $\chi_t = (75.6 \pm 2.0 \text{ MeV})^4$ . Note that this result is in tension with the LQCD results presented in Section 2.3. Given the crudeness of the instanton liquid model, we have greater confidence in the results obtained with LQCD.

## 2.5 Summary: bounds on the QCD vacuum energy

In this section, we briefly summarize the previous results. For the QCD vacuum energy (VE) defined as  $B_{2+1}^{\text{con}}$ , we have the lower bound from the GMOR relation plus the lattice (GMOR<sub>L</sub>)/sum rule average (GMOR<sub>S</sub>) derivation for the strange quark condensate (Section 2.1) plus the low-energy theorem (LET) (Section 2.2) and the upper bound from the equation of state (Section 2.3):

$$\begin{cases} (163 \text{ MeV})^4 [\text{GMOR}_L + \text{LET}] \\ (150 \text{ MeV})^4 [\text{GMOR}_S + \text{LET}] \end{cases} < \text{QCD VE} \equiv B_{2+1}^{\text{con}} < (190 \text{ MeV})^4 [\text{LQCD}_T + \text{EQCD}] . \quad (2.33)$$

Note that for reasons we will discuss in the following, we have more confidence in the GMOR<sub>L</sub> result, though we still provide the GMOR<sub>S</sub> result here for the readers' reference. For the 2-flavor quark matter property, we have also the following partial QCD vacuum energy when the strange quark condensate is nonzero and intact with

$$(119 \text{ MeV})^4 [\text{GMOR} + \text{LET}] < B_2^{\text{con}} < (160 \text{ MeV})^4 [\text{LQCD}_I + \text{pQCD} + \text{CS}] , \quad (2.34)$$

where CS stands for color superconductivity. The central value predicted by the instanton gas/liquid model (Section 2.4) is  $B_G^{\text{con}} = (196 \text{ MeV})^4$ , which is in tension with the upper bounds in Eqs. (2.33) and (2.34). In the following, as we study the stability of quark matter, we will make use of the more rigorous bounds given in Eqs. (2.33) and (2.34).

We also briefly comment on the approach of the QCD sum rules [73], which relies heavily on the approximations of the two-point spectral functions and the validity of the operator product expansion in the short-distance limit. As we have surveyed in our previous work [18] (see also Ref. [74]), there remains a huge degree of disagreement among the different sum-rule-based measurements of the gluon condensate  $\langle \alpha_s G^2 \rangle$  (see for example Ref. [75] for an overview). While the approach of the sum rules does provide a phenomenologically accessible way to study the nonperturbative properties of QCD, that its foundation is based on heuristic procedures inherently sets a limit on its potential rigor, as reflected in the example of the gluon condensate.

## 3 Quark matter stability

One immediate implication of the QCD vacuum energy is the answer to the question of quark matter stability. Quark matter could be stabilized by the balance between the quark matter pressure described by pQCD and the vacuum pressure described by the constant bag parameter  $B^{\text{con}}$ , as first proposed by Witten [6] assuming the complete restoration of the quark and gluon condensates in the quark matter phase. When the baryon chemical potential  $\mu_B$  is high, the quarks could form Cooper pairs and thus induce color superconductivity, the gap of which will also contribute to the quark matter pressure. However, due to the color factor of the antitriplet  $qq$  channel, this gap is significantly smaller than that of the color singlet  $\bar{q}q$  channel only present in the isospin-dense matter [16, 17], and its contribution has been found to be negligible in our previous analysis [18].

When the two pressures are balanced, one can then derive the corresponding energy per baryon  $\epsilon/n_B$  of the electrically neutral quark matter in the thermodynamic limit, which is in

general a function of the renormalization scale parameter  $X_\mu$  defined as

$$X_\mu = \begin{cases} \frac{\mu_R}{\frac{2}{N_c}(\mu_u + \mu_d + \mu_s)} & [2+1\text{-flavor}] \\ \frac{\mu_R}{\frac{2}{N_c}(\mu_u + 2\mu_d)} & [2\text{-flavor}] \\ \frac{\mu_R}{\mu_u - \mu_d} & [\text{isospin-dense}] \end{cases}, \quad (3.1)$$

(do not confuse it with the  $X_T$  defined with respect to  $T$  in Section 2.3),  $B^{\text{con}}$ , and  $N_f$ . If  $\epsilon/n_B \leq 930$  MeV, the averaged mass per nucleon of the iron element, then the quark matter is stable in the thermodynamic limit.<sup>5</sup> As we have studied in Ref. [18], the stable 2+1-flavor quark matter is already excluded by considering the lower bound imposed by the GMOR relation (see Section 2.1), while the fate of the stable 2-flavor quark matter still relies on the value of  $B_G^{\text{con}}$  if we assume that the  $s$ -quark condensate remains intact. We show in Figure 3 the contour of  $\epsilon/n_B = 930$  MeV predicted by the 2-flavor pQCD (pQCD<sub>2</sub>) in Ref. [18] and the bounds given in Eq. (2.33). In this plot, the gray region with  $X_\mu \lesssim 1.4$  denotes where pQCD is unreliable and thus one may not be able to draw a robust conclusion. However, given the monotonically increasing behavior of pQCD<sub>2</sub> as a function of  $X_\mu$  and the large allowed value of  $B_2^{\text{con}}$ , the balanced quark matter system should prefer  $X_\mu > 1.4$ . On the other hand, though we do not show on the plot, the pQCD<sub>2</sub> curve actually intersects with the GMOR+LET curve at  $X_\mu = 3.10$ , and thus the 2-flavor quark matter can still be stable for  $X_\mu \geq 3.10$ . However, the existence of a system with such a large renormalization scale compared to the physical scale is questionable, as supported by its inconsistency with the preferred range of  $1.47 < X_\mu < 2.09$  (vertical dashed red lines) by the LQCD<sub>I</sub> data analyzed in Ref. [18]. Therefore, the exclusion of the stable 2-flavor quark matter based on our study is robust.

In Figure 4, we also show the predicted quark matter mass per baryon or  $\epsilon/n_B$  curves for  $B_2^{\text{con}} = (119 \text{ MeV})^4$  and  $B_2^{\text{con}} = (160 \text{ MeV})^4$ , corresponding to the lower and upper bounds given in Eq. (2.34). Together with the favored range  $1.47 < X_\mu < 2.09$  based on the LQCD<sub>I</sub> data [18], we arrive at the following range for the 2-flavor quark matter mass per baryon

$$1020 \text{ MeV} < \frac{\epsilon}{n_B} < 1370 \text{ MeV}, \quad (2\text{-flavor quark matter}), \quad (3.2)$$

which clearly shows that the 2-flavor quark matter is less stable than a nucleon.

For the  $N_f = 2+1$ -flavor quark matter, we show the corresponding  $\epsilon/n_B = 930$  MeV contour in Figure 5 together with the bounds on  $B_{2+1}^{\text{con}}$  from Eq. (2.33). Similar to the 2-flavor quark matter case, the stable 2+1-flavor quark matter is also excluded. In Figure 6, we show the mass per baryon for the 2+1-flavor quark matter as a function of  $X_\mu$ . Within the preferred range of  $X_\mu$  from analyzing the LQCD<sub>I</sub> data, the 2+1-flavor quark matter has mass per baryon of

$$1130 \text{ MeV} < \frac{\epsilon}{n_B} < 1320 \text{ MeV}, \quad (2+1\text{-flavor quark matter}), \quad (3.3)$$

which is also heavier than the nucleon mass.

---

<sup>5</sup>Finite-size effects will further lower the stability of the quark nuggets, since they will increase the total energy through surface tension, etc..

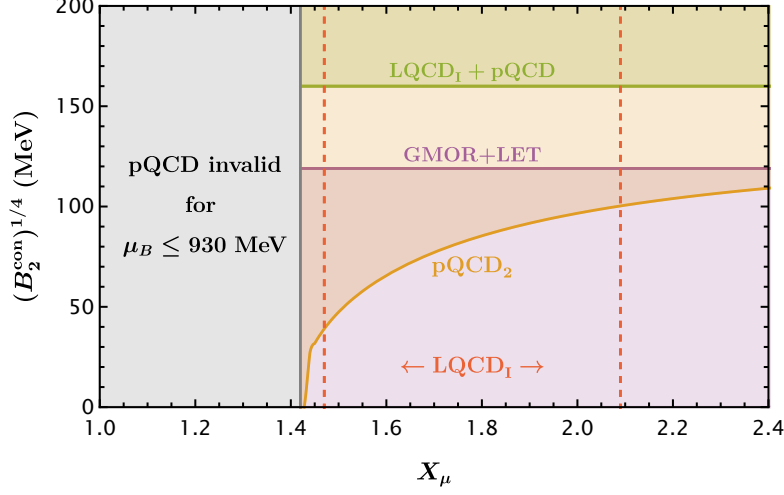


Figure 3: The  $\epsilon/n_B = 930$  MeV contour (orange) predicted by the 2-flavor pQCD (pQCD<sub>2</sub>) on the  $[X_\mu, (B_2^{\text{con}})^{1/4}]$  plane [18]. The green and purple horizontal lines are the bounds on  $B_2^{\text{con}}$  in Eq. (2.34). pQCD is invalid for  $\mu_B < 930$  MeV in the gray shaded region. The region between the two red dashed lines mark the favored  $X_\mu$  range by the LQCD<sub>I</sub> data analyzed in Ref. [18]. Note that the pQCD<sub>2</sub> curve intersects with the GMOR+LET line at  $X_\mu = 3.10$ , which is beyond the usual range of the renormalization scale choices and far from the LQCD<sub>I</sub>-preferred range.

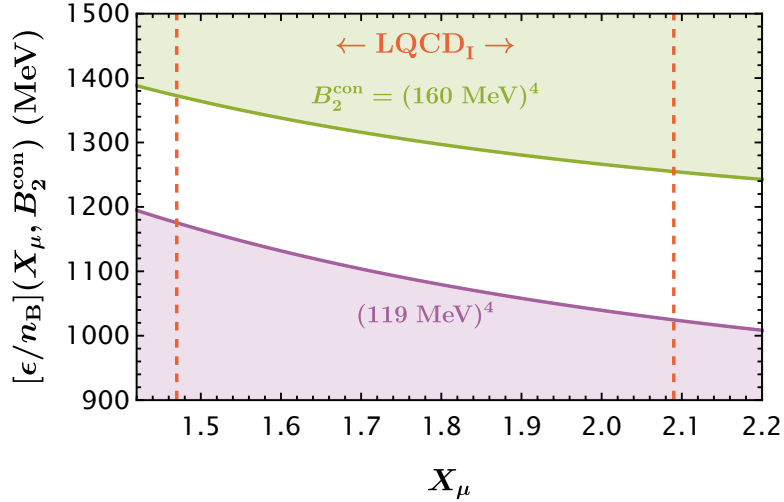


Figure 4: The 2-flavor quark matter mass per baryon or  $[\epsilon/n_B](X, B_2^{\text{con}})$  as a function of  $X_\mu$  for  $B_2^{\text{con}} = (119 \text{ MeV})^4$  and  $B_2^{\text{con}} = (160 \text{ MeV})^4$ , corresponding to the bounds given in Eq. (2.34). The region between the two vertical red dashed lines denotes the combined favored  $X_\mu$  range by the LQCD<sub>I</sub> data [18].

We note that the previous arguments were made based on the assumption that the gluon and quark condensates are totally restored in the quark matter phase or that there is a first-order phase transition when  $\mu_B$  is above some critical value. In reality, this might not necessarily be true in a dense environment, as suggested in Refs. [21, 76, 77]. The partial restoration of the condensates (especially the gluon condensate, since we are studying the quark matter) could

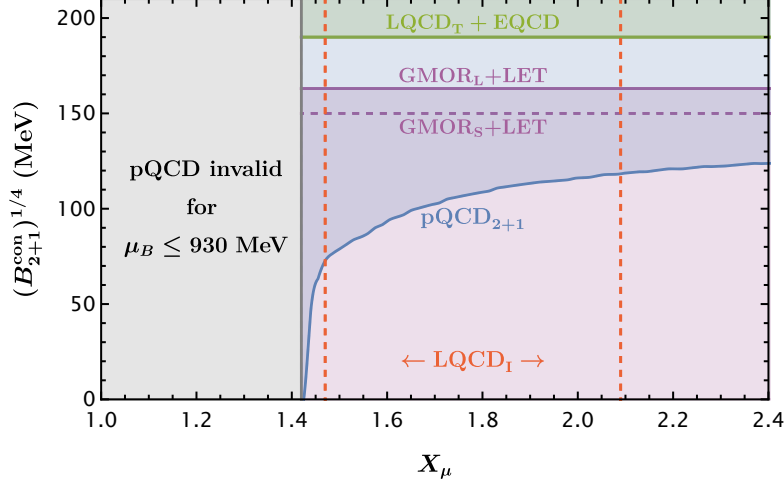


Figure 5: The  $\epsilon/n_B = 930$  MeV contour (blue) predicted by the 2+1-flavor pQCD (pQCD<sub>2+1</sub>) on the  $[X_\mu, (B_{2+1}^{\text{con}})^{1/4}]$  plane [18]. The horizontal green and purple lines show the bounds on  $B_{2+1}^{\text{con}}$  given in Eq. (2.33). pQCD is invalid for  $\mu_B < 930$  MeV in the gray shaded region. The region between the two vertical red dashed lines marks the favored  $X_\mu$  range by the LQCD<sub>I</sub> data analyzed in Ref. [18].

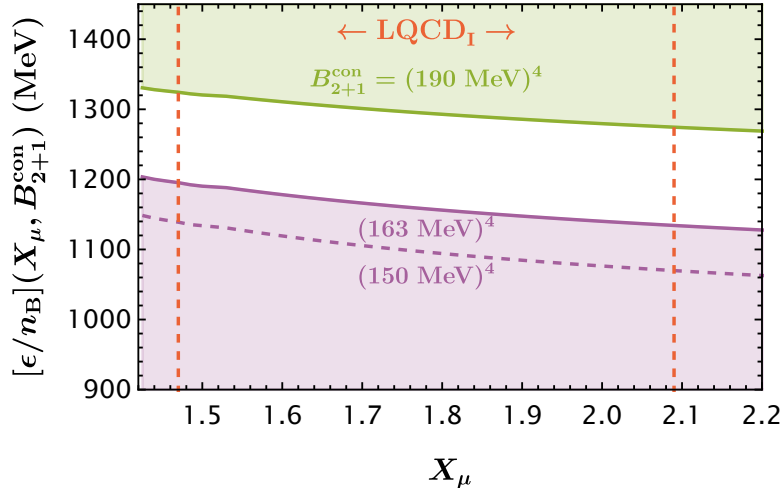


Figure 6: The 2+1-flavor quark matter mass per baryon or  $[\epsilon/n_B](X, B_{2+1}^{\text{con}})$  as a function of  $X_\mu$  for  $B_{2+1}^{\text{con}} = (150 \text{ MeV})^4$ ,  $(163 \text{ MeV})^4$ , and  $(190 \text{ MeV})^4$ , corresponding to the bounds given in Eq. (2.33). The region between the two vertical red dashed lines denotes the combined favored  $X_\mu$  range by the LQCD<sub>I</sub> data [18].

potentially reduce the vacuum pressure and allow the existence of stable “quark matter”. On the other hand, the quark energy inside a partially deconfined environment could be higher than that in a completely deconfined phase, so the quark matter may not become more stable in this intermediate situation. Nevertheless, we are not able to rely on the existing pQCD to calculate the corresponding thermodynamic properties in this case, since pQCD is only well established in the completely deconfined and chiral-symmetric phase. One possibility is to consider the quark matter pressure in an instanton background (see Ref. [78] for a review of such studies in the



context of the Nambu-Jona-Lasinio model), but it might not be able to capture the complete structure of the nonperturbative QCD vacuum, and thus so far we do not know how to answer this question in a rigorous manner.

## 4 Discussion and conclusions

Another possible though indirect way to investigate the QCD vacuum energy is through studying the Polyakov loop at finite chemical potential and/or temperature (see Ref. [79] for an example of studying it using the  $SU(N_c)$  matrix model). In pure  $SU(N_c)$  Yang-Mills theory, the order parameter of the center symmetry  $Z_{N_c}$  is the gauge-invariant Polyakov loop  $\ell_{N_c} \equiv \text{Tr}(\mathbf{L})/N_c$  with  $\mathbf{L}$  as the Wilson line in the fundamental representation. One can construct a corresponding  $Z_{N_c}$ -symmetric effective potential to study the thermodynamic properties of the gluon fields, such as [79]

$$V_{\mathbf{L}}(\ell_{N_c}, \ell_{N_c}^*) = -m^2 |\ell_{N_c}|^2 + V_{\text{vdm}}(\ell_{N_c}, \ell_{N_c}^*) , \quad (4.1)$$

where  $V_{\text{vdm}}$  is the so-called Vandermonde potential resulted from the  $SU(N_c)$  Haar measure in the path integral [79], which will restrict  $\ell_{N_c} \in [0, 1]$  as required by its definition. Once quarks are involved in the theory (such as the real-world QCD), the  $Z_{N_c}$  symmetry is then explicitly broken, which can be described by a simple tadpole interaction such as

$$V_q(\ell_{N_c}, \ell_{N_c}^*) = -\frac{h}{2} (e^{\mu/\Lambda} \ell_{N_c} + e^{-\mu/\Lambda} \ell_{N_c}^*) , \quad (4.2)$$

where  $h$  is the coupling strength,  $\mu$  is the chemical potential, and  $\Lambda$  is some reference energy scale. By examining the vacuum structure of  $V_{\text{eff}} \equiv V_{\mathbf{L}} + V_q$ , one finds that the vacuum expectation values  $\langle \ell_{N_c} \rangle$  and  $\langle \ell_{N_c}^* \rangle$  as well as the vacuum energy  $V_{\text{eff}}(\langle \ell_{N_c} \rangle, \langle \ell_{N_c}^* \rangle)$  are all functions of  $\mu$ . Although the gluon condensate in real QCD is not a good order parameter (not associated with a good symmetry) of the theory (and thus of the already broken center symmetry), its close relation to  $\ell_{N_c}$  through the gluon dynamics hints at the possibility of gradual restoration of the gluon condensate with increasing quark matter density. While so far, at least to our knowledge, there is no literature that explores this direction, it could serve as a complementary approach to study the quark matter in a partially restored vacuum to the instanton background picture briefly mentioned in Section 3.

Even though we have excluded the existence of stable quark matter (with the possible caveat of its existence in a partially deconfined phase), it is a logical question to ask whether quark matter or a quark nugget can be a long-lived state capable of surviving through the age of the universe. One could use the picture of quantum tunneling, similar to the  $\alpha$  decay of certain nuclei, to estimate the decay rate or lifetime of a quark nugget. The decay rate is anticipated to have an exponential suppression factor of  $e^{-d\sqrt{2m(V-E)}}$ , with  $d \sim (100 \text{ MeV})^{-1}$  representing the surface thickness of the quark nugget,  $V$  the height of the potential barrier, and  $E$  the emitting baryon energy with a mass  $m$ . Note that if the quark matter state were globally stable ( $E < 0$ ) or metastable ( $E \sim 0$ ), as opposed to our conclusion, then the tunneling would either be prohibited or highly suppressed. For large quark nuggets, the total mass consists of the bulk contribution of  $\sim AB^{1/4}$  and the surface contribution of  $\sim A^{2/3} B^{1/4}$ . The binding energy, or  $V - E$ , for a small quark nugget bound by a large quark nugget is estimated to be  $O(B^{1/4})$ .

Since  $B^{1/4}$  and  $1/d$  are both  $\sim O(100 \text{ MeV})$ , there is no large exponential factor to suppress the decay rate. Hence, we conclude that quark nuggets are short-lived.

Another possible mechanism to stabilize the quark nuggets is to introduce new physics that can either supply additional charges beyond the baryon number to account for Q-ball stability or an additional order-parameter potential that changes the energy configuration of the quark matter. Some examples are a scalar field that interacts with the topological sector of QCD and leads to the formation of domain walls (see for instance Ref. [80]) and the “axion quark nuggets” [81]. These new physics are well motivated not only for their potential contribution to the stability of the quark nuggets, but also for the possible production mechanism of the quark nuggets in the early universe that they can provide, in contrast to the smooth QCD crossover in the Standard Model QCD [57, 58].

In addition to the stability of quark matter, the QCD vacuum energy between  $(163 \text{ MeV})^4$  and  $(190 \text{ MeV})^4$  is also an important factor in the study of (hybrid) neutron stars. For a neutron star with a dense enough core, it is expected that the core matter will exist in the form of deconfined quarks. As the transition from ordinary hadron matter to deconfined quark matter in a cold baryon-dense environment is expected to be first-order, the associated latent heat will greatly affect the stability of the quark matter core and is responsible for the existence of stable hybrid stars. One such limit derived from the perturbation of a small compact core is called the Seidov limit [82], while there are also several studies on the stability of hybrid stars with a macroscopic quark core (see for example Refs. [83, 84]). Moreover, the resulted equation of state of the cold baryon matter will also determine the properties of the hybrid stars (see for example Refs. [85, 86]). Since the QCD vacuum energy plays a major role in the properties of the phase transition, the content explored in this paper will be useful for future studies of neutron star properties.

Last but not least, the precise value of the QCD vacuum energy could also be important for the Cosmological Constant (CC) Problem [20, 87, 88]. The cosmological constant in the current universe is  $(2.25 \times 10^{-3} \text{ eV})^4$  [89], which is  $(2.0, 3.6) \times 10^{-44}$  of the QCD vacuum energy bounds derived in this study. Given that the QCD phase transition is the last known phase transition to modify the vacuum energy, any dynamical solution to the CC problem is likely to be concerned with QCD and possibly the precise value of the QCD vacuum energy. On the other hand, a solution based on the landscape of multiple vacua is unlikely to care about its precise value.

In conclusion, the nonperturbative QCD vacuum energy has been studied in the language of the QCD trace anomaly, with a focus on the completely deconfined and chiral-symmetric phase that is parametrized by the  $T$ - and  $\mu$ -independent  $B^{\text{con}}$ . We have adopted several approaches, including the GMOR relation, the low-energy theorem plus the LQCD measurement for the topological susceptibility, the fits to the equations of state from the LQCD<sub>T</sub> and LQCD<sub>I</sub> calculations, and the instanton gas/liquid model, to obtain both the lower and upper bounds on the QCD vacuum energy. The QCD vacuum energy is constrained within a small range of  $(163 \text{ MeV})^4 < \text{QCD VE} < (190 \text{ MeV})^4$ . Using the completely deconfined and chiral-symmetry restored picture and the bounds on the QCD vacuum energy, we have excluded both the stable 2+1- and 2-flavor quark matter. Therefore, we have come close to answering the half-century question of the stability of quark matter, as proposed by both Bodmer and Witten. Based on our findings, we have now excluded the possibility of stable quark matter.

## Acknowledgments

This work is supported by the U.S. Department of Energy under the contract DE-SC-0017647. YB is also supported by the U.S. Department of Energy under contracts No. DEAC02-06CH11357 at Argonne National Laboratory. TKC is also supported by the Ministry of Education, Taiwan, under the Government Scholarship to Study Abroad.

## A EQCD formulas for the quark-gluon plasma pressure

We recap in this section the formulas of EQCD for the pressure of the quark-gluon plasma at a finite temperature  $T$  from Refs. [12, 13]. For a system of  $N_f$  massless quark flavors with  $N_c = 3$  and the renormalization scale  $\bar{\mu}$ , the pressure  $p_{\text{QCD},0}(\bar{\mu}, T, \Delta)$  is given up to  $\mathcal{O}(g^6 \ln g)$  by

$$p_{\text{QCD},0}(\bar{\mu}, T, \Delta) = \frac{8\pi^2}{45} T^4 \left[ \sum_{i=0}^6 \left( \frac{\alpha_s(\bar{\mu})}{\pi} \right)^{i/2} p_i \right], \quad (\text{A.1})$$

where

$$p_0 = 1 + \frac{21}{32} N_f, \quad (\text{A.2})$$

$$p_1 = 0, \quad (\text{A.3})$$

$$p_2 = -\frac{15}{4} \left( 1 + \frac{5}{12} N_f \right), \quad (\text{A.4})$$

$$p_3 = 30 \left( 1 + \frac{1}{6} N_f \right)^{3/2}, \quad (\text{A.5})$$

$$p_4 = 237.2 + 15.96 N_f - 0.4150 N_f^2 + \frac{135}{2} \left( 1 + \frac{1}{6} N_f \right) \ln \left[ \frac{\alpha_s}{\pi} \left( 1 + \frac{1}{6} N_f \right) \right] - \frac{165}{8} \left( 1 + \frac{5}{12} N_f \right) \left( 1 - \frac{2}{33} N_f \right) \ln \frac{\bar{\mu}}{2\pi T}, \quad (\text{A.6})$$

$$p_5 = \left( 1 + \frac{1}{6} N_f \right)^{1/2} \left[ -799.1 - 21.96 N_f - 1.926 N_f^2 + \frac{495}{2} \left( 1 + \frac{1}{6} N_f \right) \left( 1 - \frac{2}{33} N_f \right) \ln \frac{\bar{\mu}}{2\pi T} \right], \quad (\text{A.7})$$

$$p_6 = \left[ -659.2 - 65.89 N_f - 7.653 N_f^2 + \frac{1485}{2} \left( 1 + \frac{1}{6} N_f \right) \left( 1 - \frac{2}{33} N_f \right) \ln \frac{\bar{\mu}}{2\pi T} \right] \ln \left[ \frac{\alpha_s}{\pi} \left( 1 + \frac{1}{6} N_f \right) \right] - 475.6 \ln \frac{\alpha_s}{\pi} - \frac{1815}{16} \left( 1 + \frac{5}{12} N_f \right) \left( 1 - \frac{2}{33} N_f \right)^2 \ln^2 \frac{\bar{\mu}}{2\pi T} + (2932.9 + 42.83 N_f - 16.48 N_f^2 + 0.2767 N_f^3) \frac{\bar{\mu}}{2\pi T} + \Delta(N_f), \quad (\text{A.8})$$

with  $\Delta$  being an unknown constant to be fit. In our study, we define the renormalization scale parameter  $X_T \equiv \bar{\mu}/(2\pi T)$ . We consider the running of  $\alpha_s$  and  $m_s$  up to  $\mathcal{O}(\alpha_s^2)$ ,

$$\alpha_s(\bar{\mu}) = \frac{4\pi}{\beta_0 L} \left( 1 - \frac{2\beta_1 \ln L}{\beta_0^2 L} \right), \quad \text{with } L = \ln(\bar{\mu}^2/\Lambda_{\overline{\text{MS}}}^2), \quad (\text{A.9})$$

$$m_s(\bar{\mu}) = m_s(2 \text{ GeV}) \left( \frac{\alpha_s(\bar{\mu})}{\alpha_s(2 \text{ GeV})} \right)^{\gamma_0/\beta_0} \times \frac{1 + A_1 \frac{\alpha_s(\bar{\mu})}{\pi} + \frac{A_1^2 + A_2}{2} \left( \frac{\alpha_s(\bar{\mu})}{\pi} \right)^2}{1 + A_1 \frac{\alpha_s(2 \text{ GeV})}{\pi} + \frac{A_1^2 + A_2}{2} \left( \frac{\alpha_s(2 \text{ GeV})}{\pi} \right)^2}, \quad (\text{A.10})$$

where we choose  $\Lambda_{\overline{\text{MS}}} = 378 \text{ MeV}$ ,  $m_s(2 \text{ GeV}) = 93.5 \text{ MeV}$ , and

$$A_1 = -\frac{\beta_1 \gamma_0}{2\beta_0^2} + \frac{\gamma_1}{4\beta_0}, \quad A_2 = \frac{\gamma_0}{4\beta_0^2} \left( \frac{\beta_1^2}{\beta_0} - \beta_2 \right) - \frac{\beta_1 \gamma_1}{8\beta_0^2} + \frac{\gamma_2}{16\beta_0}. \quad (\text{A.11})$$

The  $SU(3)_C$  group theory factors as well as the  $\beta_i$  and  $\gamma_j$  factors are summarized as follows:

$$\begin{aligned} d_A &= N_c^2 - 1, & C_A &= N_c, & C_F &= \frac{N_c^2 - 1}{2N_c}, \\ \beta_0 &= \frac{11C_A - 2N_f}{3}, & \beta_1 &= \frac{17}{3}C_A^2 - C_F N_f - \frac{5}{3}C_A N_f, \\ \beta_2 &= \frac{2857}{216}C_A^3 + \frac{1}{4}C_F^2 N_f - \frac{205}{72}C_A C_F N_f - \frac{1415}{216}C_A^2 N_f + \frac{11}{36}C_F N_f^2 + \frac{79}{216}C_A N_f^2, \\ \gamma_0 &= 3C_F, & \gamma_1 &= C_F \left( \frac{97}{6}C_A + \frac{3}{2}C_F - \frac{5}{3}N_f \right), \\ \gamma_2 &= C_F \left\{ \frac{129}{2}C_F^2 - \frac{129}{4}C_F C_A + \frac{11413}{108}C_A^2 + C_F N_f [-23 + 24\zeta(3)] \right. \\ &\quad \left. + C_A N_f \left[ -\frac{278}{27} - 24\zeta(3) \right] - \frac{35}{27}N_f^2 \right\}. \end{aligned} \quad (\text{A.12})$$

The massive quark effects are only included up to  $\mathcal{O}(g^2)$  in Ref. [13] by modifying  $p_{\text{QCD},0}$  by

$$p_{\text{QCD},m}(N_f, \bar{\mu}, T, \Delta) \equiv \frac{\left[ \alpha_{E1}^{\overline{\text{MS}}} + g^2 \alpha_{E2}^{\overline{\text{MS}}} \right] (N_f)}{\left[ \alpha_{E1}^{\overline{\text{MS}}} + g^2 \alpha_{E2}^{\overline{\text{MS}}} \right] (0)} \times p_{\text{QCD},0}(\bar{\mu}, T, \Delta), \quad (\text{A.13})$$

where

$$\alpha_{E1}^{\overline{\text{MS}}} = d_A \frac{\pi^2}{45} + 4C_A \sum_{i=1}^{N_f} F_1 \left( \frac{m_i^2}{T^2} \right), \quad (\text{A.14})$$

$$\begin{aligned} \alpha_{E2}^{\overline{\text{MS}}} &= -\frac{d_A C_A}{144} - d_A \sum_{i=1}^{N_f} \left\{ \frac{1}{6} F_2 \left( \frac{m_i^2}{T^2} \right) \left[ 1 + 6F_2 \left( \frac{m_i^2}{T^2} \right) \right] \right. \\ &\quad \left. + \frac{m_i^2}{4\pi^2 T^2} \left( 3 \ln \frac{\bar{\mu}}{m_i} + 2 \right) F_2 \left( \frac{m_i^2}{T^2} \right) - \frac{2m_i^2}{T^2} F_4 \left( \frac{m_i^2}{T^2} \right) \right\}, \end{aligned} \quad (\text{A.15})$$

with

$$F_1(y) = \frac{1}{12\pi^2} \int_0^\infty dx \left( \frac{x}{x+y} \right)^{1/2} n_F(\sqrt{x+y}) x, \quad (\text{A.16})$$

$$F_2(y) = \frac{1}{4\pi^2} \int_0^\infty dx \left( \frac{x}{x+y} \right)^{1/2} n_F(\sqrt{x+y}), \quad (\text{A.17})$$

$$F_4(y) = \frac{2}{(4\pi)^4} \int_0^\infty dx_1 \int_0^\infty dx_2 \frac{1}{\sqrt{x_1+y}\sqrt{x_2+y}} n_F(\sqrt{x_1+y}) n_F(\sqrt{x_2+y}) \\ \times \ln \left[ \frac{\sqrt{x_1+y}\sqrt{x_2+y} + y - \sqrt{x_1x_2}}{\sqrt{x_1+y}\sqrt{x_2+y} + y + \sqrt{x_1x_2}} \times \frac{\sqrt{x_1+y}\sqrt{x_2+y} - y + \sqrt{x_1x_2}}{\sqrt{x_1+y}\sqrt{x_2+y} - y - \sqrt{x_1x_2}} \right], \quad (\text{A.18})$$

and  $n_F(x) = 1/(e^x + 1)$ . Finally, we include the bag parameter  $B$  and obtain the total pressure

$$p_{\text{QCD}}(N_f, \bar{\mu}, T, \Delta, B) = p_{\text{QCD,m}}(N_f, \bar{\mu}, T, \Delta) - B. \quad (\text{A.19})$$

## B Bag parameter inference in the hot $SU(3)$ theory

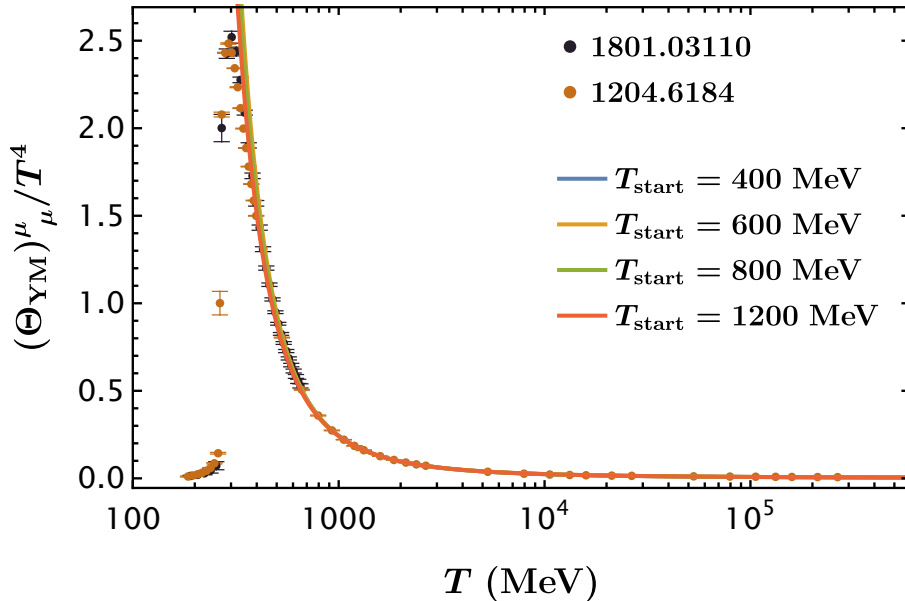


Figure 7: The lattice trace anomaly data of the hot pure  $SU(3)$  Yang-Mills model from Refs. [61, 62], as well as the best-fit curves with  $T_{\text{start}} = 400, 600, 800, 1200$  MeV. Note that the phase transition temperature  $T_c \approx 270$  MeV.

We present the details of the pure  $SU(3)$  gauge theory lattice study [61, 62] in this section. As in the case of the LQCD<sub>T</sub> study, the quantity we choose to fit is the normalized trace anomaly  $(\Theta_{\text{YM}})^\mu_\mu / T^4 = T \partial(p_{\text{YM}}/T^4) / \partial T$ . Different from real-world QCD, however, the phase transition of the  $SU(3)$  theory is first-order, and there is an additional “fuzzy bag parameter ( $2B_{\text{fuzzy}}T^2 \subset (\Theta_{\text{YM}})^\mu_\mu$ ) [90]” to the traditional bag parameter  $B_{\text{YM}}$ , the latter as in the MIT bag model [91, 92]. By setting  $N_f = 0$  in the EQCD formulas, one has

$$p_{\text{YM}}(T, X_T, \Delta, B_{\text{fuzzy}}, B_{\text{YM}}) = p_{\text{QCD},0}(2\pi T X_T, T, \Delta) - B_{\text{fuzzy}}T^2 - B_{\text{YM}}, \quad (\text{B.1})$$

which contains four parameters to be fit:  $X_T$ ,  $\Delta$ ,  $B_{\text{fuzzy}}$ , and  $B_{\text{YM}}$ . With  $T_c \approx 270$  MeV (which also determines the reference scale  $\Lambda_{\overline{\text{MS}}} \approx 1.26 T_c$  [61]), we choose  $T_{\text{start}} = 400, 600, 800, 1200$  MeV, whose numbers of the degrees of freedom  $k$  and best-fit parameters are given by

$$\begin{aligned}
T_{\text{start}} = 400 \text{ MeV} & : (k, \chi^2, X_T, \Delta, B_{\text{fuzzy}}^{1/2}, B_{\text{YM}}^{1/4}) = (38, 34.0, 0.86, -3268, 176.3 \text{ MeV}, 246.4 \text{ MeV}) , \\
T_{\text{start}} = 600 \text{ MeV} & : (k, \chi^2, X_T, \Delta, B_{\text{fuzzy}}^{1/2}, B_{\text{YM}}^{1/4}) = (25, 16.0, 0.92, -3454, 173.9 \text{ MeV}, 259.3 \text{ MeV}) , \\
T_{\text{start}} = 800 \text{ MeV} & : (k, \chi^2, X_T, \Delta, B_{\text{fuzzy}}^{1/2}, B_{\text{YM}}^{1/4}) = (19, 14.6, 0.88, -3353, 169.2 \text{ MeV}, 251.4 \text{ MeV}) , \\
T_{\text{start}} = 1200 \text{ MeV} & : (k, \chi^2, X_T, \Delta, B_{\text{fuzzy}}^{1/2}, B_{\text{YM}}^{1/4}) = (16, 13.7, 0.88, -3341, 174.0 \text{ MeV}, 238.9 \text{ MeV}) .
\end{aligned}
\tag{B.2}$$

The optimal p-value is obtained when  $T_{\text{start}} = 600$  MeV, which is 0.915. We present the lattice data and the best-fit curves for different  $T_{\text{start}}$  values in Figure 7. Note that we are able to extract  $B_{\text{YM}}$ , in contrast to the LQCD<sub>T</sub> case, because of the smaller uncertainties in the low- $T$  regime, which, for all four choices of  $T_{\text{start}}$ , is consistently given by  $B_{\text{YM}} \lesssim T_c^4$ . In particular, for  $T_{\text{start}} = 600$  MeV, we have  $B_{\text{YM}} = 0.85 T_c^4$ .

## References

- [1] A. R. Bodmer, *Collapsed nuclei*, *Phys. Rev. D* **4** (1971) 1601–1606.
- [2] T. D. Lee, *Abnormal Nuclear States and Vacuum Excitations*, *Rev. Mod. Phys.* **47** (1975) 267–275.
- [3] T. D. Lee and M. Margulies, *Interaction of a Dense Fermion Medium with a Scalar Meson Field*, *Phys. Rev. D* **11** (1975) 1591. [Erratum: *Phys.Rev.D* 12, 4008 (1975)].
- [4] R. Friedberg and T. D. Lee, *Fermion Field Nontopological Solitons. 1.*, *Phys. Rev. D* **15** (1977) 1694.
- [5] R. Friedberg and T. D. Lee, *Fermion Field Nontopological Solitons. 2. Models for Hadrons*, *Phys. Rev. D* **16** (1977) 1096.
- [6] E. Witten, *Cosmic Separation of Phases*, *Phys. Rev. D* **30** (1984) 272–285.
- [7] Y. Bai and M. Korwar, *Radioactivity of Quark Nuggets*, [arXiv:2409.16487](https://arxiv.org/abs/2409.16487).
- [8] A. Kurkela, P. Romatschke, and A. Vuorinen, *Cold Quark Matter*, *Phys. Rev. D* **81** (2010) 105021, [[arXiv:0912.1856](https://arxiv.org/abs/0912.1856)].
- [9] A. Kärkkäinen, P. Navarrete, M. Nurmela, R. Paatelainen, K. Seppänen, and A. Vuorinen, *Quark matter at four loops: hardships and how to overcome them*, [arXiv:2501.17921](https://arxiv.org/abs/2501.17921).
- [10] T. Appelquist and R. D. Pisarski, *High-Temperature Yang-Mills Theories and Three-Dimensional Quantum Chromodynamics*, *Phys. Rev. D* **23** (1981) 2305.
- [11] S. Nadkarni, *Dimensional Reduction in Hot QCD*, *Phys. Rev. D* **27** (1983) 917.
- [12] K. Kajantie, M. Laine, K. Rummukainen, and Y. Schroder, *The Pressure of hot QCD up to  $g_6 \ln(1/g)$* , *Phys. Rev. D* **67** (2003) 105008, [[hep-ph/0211321](https://arxiv.org/abs/hep-ph/0211321)].
- [13] M. Laine and Y. Schroder, *Quark mass thresholds in QCD thermodynamics*, *Phys. Rev. D* **73** (2006) 085009, [[hep-ph/0603048](https://arxiv.org/abs/hep-ph/0603048)].

- [14] A. D. Linde, *Infrared Problem in Thermodynamics of the Yang-Mills Gas*, *Phys. Lett. B* **96** (1980) 289–292.
- [15] D. J. Gross, R. D. Pisarski, and L. G. Yaffe, *QCD and Instantons at Finite Temperature*, *Rev. Mod. Phys.* **53** (1981) 43.
- [16] Y. Fujimoto, *Enhanced contribution of the pairing gap to the QCD equation of state at large isospin chemical potential*, *Phys. Rev. D* **109** (2024), no. 5 054035, [[arXiv:2312.11443](#)].
- [17] Y. Fujimoto, *Interplay between the weak-coupling results and the lattice data in dense QCD*, [arXiv:2408.12514](#).
- [18] Y. Bai and T.-K. Chen, *Approaching Stable Quark Matter*, [arXiv:2410.19678](#).
- [19] M. Gell-Mann, R. J. Oakes, and B. Renner, *Behavior of current divergences under  $SU(3)$   $\times$   $SU(3)$* , *Phys. Rev.* **175** (1968) 2195–2199.
- [20] J. F. Donoghue, *The Multiverse and Particle Physics*, *Ann. Rev. Nucl. Part. Sci.* **66** (2016) 1–21, [[arXiv:1601.05136](#)].
- [21] V. A. Novikov, M. A. Shifman, A. I. Vainshtein, and V. I. Zakharov, *Are All Hadrons Alike?*, *Nucl. Phys. B* **191** (1981) 301–369.
- [22] S. Borsanyi et al., *Calculation of the axion mass based on high-temperature lattice quantum chromodynamics*, *Nature* **539** (2016), no. 7627 69–71, [[arXiv:1606.07494](#)].
- [23] R. Abbott, W. Detmold, M. Illa, A. Parreño, R. J. Perry, F. Romero-López, P. E. Shanahan, and M. L. Wagman, *QCD constraints on isospin-dense matter and the nuclear equation of state*, [arXiv:2406.09273](#).
- [24] S. Borsanyi, Z. Fodor, C. Hoelbling, S. D. Katz, S. Krieg, and K. K. Szabo, *Full result for the QCD equation of state with 2+1 flavors*, *Phys. Lett. B* **730** (2014) 99–104, [[arXiv:1309.5258](#)].
- [25] **HotQCD** Collaboration, A. Bazavov et al., *Equation of state in (2+1)-flavor QCD*, *Phys. Rev. D* **90** (2014) 094503, [[arXiv:1407.6387](#)].
- [26] A. Bazavov, P. Petreczky, and J. H. Weber, *Equation of State in 2+1 Flavor QCD at High Temperatures*, *Phys. Rev. D* **97** (2018), no. 1 014510, [[arXiv:1710.05024](#)].
- [27]  **$\chi$ QCD** Collaboration, B. Wang, F. He, G. Wang, T. Draper, J. Liang, K.-F. Liu, and Y.-B. Yang, *Trace anomaly form factors from lattice QCD*, *Phys. Rev. D* **109** (2024), no. 9 094504, [[arXiv:2401.05496](#)].
- [28] B. Hu, X. Jiang, K.-F. Liu, P. Sun, and Y.-B. Yang, *Trace anomaly contributions to baryon masses from Lattice QCD*, [arXiv:2411.18402](#).
- [29] T. D. Cohen, R. J. Furnstahl, and D. K. Griegel, *Quark and gluon condensates in nuclear matter*, *Phys. Rev. C* **45** (1992) 1881–1893.
- [30] L. He, Y. Jiang, and P. Zhuang, *Quark and Gluon Condensates in Isospin Matter*, *Phys. Rev. C* **79** (2009) 045205, [[arXiv:0812.0237](#)].
- [31] B. Holdom, J. Ren, and C. Zhang, *Quark matter may not be strange*, *Phys. Rev. Lett.* **120** (2018), no. 22 222001, [[arXiv:1707.06610](#)].
- [32] A. M. Polyakov, *Thermal Properties of Gauge Fields and Quark Liberation*, *Phys. Lett. B* **72** (1978) 477–480.

- [33] J. C. Collins, A. Duncan, and S. D. Joglekar, *Trace and Dilatation Anomalies in Gauge Theories*, *Phys. Rev. D* **16** (1977) 438–449.
- [34] N. K. Nielsen, *The Energy Momentum Tensor in a Nonabelian Quark Gluon Theory*, *Nucl. Phys. B* **120** (1977) 212–220.
- [35] Y. Hatta, A. Rajan, and K. Tanaka, *Quark and gluon contributions to the QCD trace anomaly*, *JHEP* **12** (2018) 008, [[arXiv:1810.05116](https://arxiv.org/abs/1810.05116)].
- [36] S. Borsanyi, S. Durr, Z. Fodor, S. Krieg, A. Schafer, E. E. Scholz, and K. K. Szabo, *SU(2) chiral perturbation theory low-energy constants from 2+1 flavor staggered lattice simulations*, *Phys. Rev. D* **88** (2013) 014513, [[arXiv:1205.0788](https://arxiv.org/abs/1205.0788)].
- [37] **Particle Data Group** Collaboration, S. Navas et al., *Review of particle physics*, *Phys. Rev. D* **110** (2024), no. 3 030001.
- [38] C. McNeile, A. Bazavov, C. T. H. Davies, R. J. Dowdall, K. Hornbostel, G. P. Lepage, and H. D. Trottier, *Direct determination of the strange and light quark condensates from full lattice QCD*, *Phys. Rev. D* **87** (2013), no. 3 034503, [[arXiv:1211.6577](https://arxiv.org/abs/1211.6577)].
- [39] S. Narison, *QCD as a Theory of Hadrons: From Partons to Confinement*. Cambridge University Press, 2004.
- [40] K. G. Chetyrkin, *Quark mass anomalous dimension to  $O(\alpha_s^4)$* , *Phys. Lett. B* **404** (1997) 161–165, [[hep-ph/9703278](https://arxiv.org/abs/hep-ph/9703278)].
- [41] M. A. Shifman, A. I. Vainshtein, and V. I. Zakharov, *Can Confinement Ensure Natural CP Invariance of Strong Interactions?*, *Nucl. Phys. B* **166** (1980) 493–506.
- [42] **TWQCD** Collaboration, Y.-Y. Mao and T.-W. Chiu, *Topological Susceptibility to the One-Loop Order in Chiral Perturbation Theory*, *Phys. Rev. D* **80** (2009) 034502, [[arXiv:0903.2146](https://arxiv.org/abs/0903.2146)].
- [43] S. Aoki and H. Fukaya, *Chiral perturbation theory in a theta vacuum*, *Phys. Rev. D* **81** (2010) 034022, [[arXiv:0906.4852](https://arxiv.org/abs/0906.4852)].
- [44] F.-K. Guo and U.-G. Meißner, *Cumulants of the QCD topological charge distribution*, *Phys. Lett. B* **749** (2015) 278–282, [[arXiv:1506.05487](https://arxiv.org/abs/1506.05487)].
- [45] **JLQCD** Collaboration, S. Aoki, G. Cossu, H. Fukaya, S. Hashimoto, and T. Kaneko, *Topological susceptibility in 2+1-flavor QCD with chiral fermions*, *EPJ Web Conf.* **175** (2018) 04008, [[arXiv:1712.05541](https://arxiv.org/abs/1712.05541)].
- [46] **NPLQCD** Collaboration, R. Abbott, W. Detmold, F. Romero-López, Z. Davoudi, M. Illa, A. Parreño, R. J. Perry, P. E. Shanahan, and M. L. Wagman, *Lattice quantum chromodynamics at large isospin density*, *Phys. Rev. D* **108** (2023), no. 11 114506, [[arXiv:2307.15014](https://arxiv.org/abs/2307.15014)].
- [47] E. V. Shuryak, *Theory of Hadronic Plasma*, *Sov. Phys. JETP* **47** (1978) 212–219.
- [48] S. A. Chin, *Transition to Hot Quark Matter in Relativistic Heavy Ion Collision*, *Phys. Lett. B* **78** (1978) 552–555.
- [49] J. I. Kapusta, *Quantum Chromodynamics at High Temperature*, *Nucl. Phys. B* **148** (1979) 461–498.
- [50] T. Toimela, *The Next Term in the Thermodynamic Potential of QCD*, *Phys. Lett. B* **124** (1983) 407–409.



- [51] P. B. Arnold and C.-X. Zhai, *The Three loop free energy for pure gauge QCD*, *Phys. Rev. D* **50** (1994) 7603–7623, [[hep-ph/9408276](#)].
- [52] P. B. Arnold and C.-x. Zhai, *The Three loop free energy for high temperature QED and QCD with fermions*, *Phys. Rev. D* **51** (1995) 1906–1918, [[hep-ph/9410360](#)].
- [53] C.-x. Zhai and B. M. Kastening, *The Free energy of hot gauge theories with fermions through  $g^{*5}$* , *Phys. Rev. D* **52** (1995) 7232–7246, [[hep-ph/9507380](#)].
- [54] A. Hietanen, K. Kajantie, M. Laine, K. Rummukainen, and Y. Schroder, *Plaquette expectation value and gluon condensate in three dimensions*, *JHEP* **01** (2005) 013, [[hep-lat/0412008](#)].
- [55] F. Di Renzo, M. Laine, V. Miccio, Y. Schroder, and C. Torrero, *The Leading non-perturbative coefficient in the weak-coupling expansion of hot QCD pressure*, *JHEP* **07** (2006) 026, [[hep-ph/0605042](#)].
- [56] P. Navarrete and Y. Schröder, *The  $g^6$  pressure of hot Yang-Mills theory: canonical form of the integrand*, *JHEP* **11** (2024) 037, [[arXiv:2408.15830](#)].
- [57] Y. Aoki, G. Endrodi, Z. Fodor, S. D. Katz, and K. K. Szabo, *The Order of the quantum chromodynamics transition predicted by the standard model of particle physics*, *Nature* **443** (2006) 675–678, [[hep-lat/0611014](#)].
- [58] T. Bhattacharya et al., *QCD Phase Transition with Chiral Quarks and Physical Quark Masses*, *Phys. Rev. Lett.* **113** (2014), no. 8 082001, [[arXiv:1402.5175](#)].
- [59] R. A. Schneider, *The QCD running coupling at finite temperature and density*, [[hep-ph/0303104](#)].
- [60] M. Bresciani, M. D. Brida, L. Giusti, and M. Pepe, *The QCD Equation of State with  $N_f = 3$  flavours up to the electro-weak scale*, [[arXiv:2501.11603](#)].
- [61] S. Borsanyi, G. Endrodi, Z. Fodor, S. D. Katz, and K. K. Szabo, *Precision  $SU(3)$  lattice thermodynamics for a large temperature range*, *JHEP* **07** (2012) 056, [[arXiv:1204.6184](#)].
- [62] M. Caselle, A. Nada, and M. Panero, *QCD thermodynamics from lattice calculations with nonequilibrium methods: The  $SU(3)$  equation of state*, *Phys. Rev. D* **98** (2018), no. 5 054513, [[arXiv:1801.03110](#)].
- [63] T. Schäfer and E. V. Shuryak, *The Interacting instanton liquid in QCD at zero and finite temperature*, *Phys. Rev. D* **53** (1996) 6522–6542, [[hep-ph/9509337](#)].
- [64] E. V. Shuryak and T. Schäfer, *The QCD vacuum as an instanton liquid*, *Ann. Rev. Nucl. Part. Sci.* **47** (1997) 359–394.
- [65] C. Bonati, M. D’Elia, and A. Scapellato,  *$\theta$  dependence in  $SU(3)$  Yang-Mills theory from analytic continuation*, *Phys. Rev. D* **93** (2016), no. 2 025028, [[arXiv:1512.01544](#)].
- [66] G. ’t Hooft, *Computation of the Quantum Effects Due to a Four-Dimensional Pseudoparticle*, *Phys. Rev. D* **14** (1976) 3432–3450. [Erratum: *Phys. Rev. D* **18**, 2199 (1978)].
- [67] C. G. Callan, Jr., R. F. Dashen, and D. J. Gross, *Toward a Theory of the Strong Interactions*, *Phys. Rev. D* **17** (1978) 2717.
- [68] M. A. Shifman, A. I. Vainshtein, and V. I. Zakharov, *Instanton Density in a Theory with Massless Quarks*, *Nucl. Phys. B* **163** (1980) 46–56.

- [69] P. J. Moran and D. B. Leinweber, *Impact of Dynamical Fermions on QCD Vacuum Structure*, *Phys. Rev. D* **78** (2008) 054506, [[arXiv:0801.2016](#)].
- [70] T. Schäfer and E. V. Shuryak, *Instantons in QCD*, *Rev. Mod. Phys.* **70** (1998) 323–426, [[hep-ph/9610451](#)].
- [71] E. Witten, *Current Algebra Theorems for the U(1) Goldstone Boson*, *Nucl. Phys. B* **156** (1979) 269–283.
- [72] G. Veneziano, *U(1) Without Instantons*, *Nucl. Phys. B* **159** (1979) 213–224.
- [73] M. A. Shifman, A. I. Vainshtein, and V. I. Zakharov, *QCD and Resonance Physics. Theoretical Foundations*, *Nucl. Phys. B* **147** (1979) 385–447.
- [74] J. F. Donoghue, E. Golowich, and B. R. Holstein, *Dynamics of the Standard Model*. Cambridge Monographs on Particle Physics, Nuclear Physics and Cosmology. Cambridge University Press, 2 ed., 2014.
- [75] S. Narison, *QCD parameter correlations from heavy quarkonia*, *Int. J. Mod. Phys. A* **33** (2018), no. 10 1850045, [[arXiv:1801.00592](#)]. [Addendum: *Int.J.Mod.Phys.A* 33, 1892004 (2018)].
- [76] E. V. Shuryak, *Quantum Chromodynamics and the Theory of Superdense Matter*, *Phys. Rept.* **61** (1980) 71–158.
- [77] E. V. Shuryak, *The Role of Instantons in Quantum Chromodynamics. 3. Quark - Gluon Plasma*, *Nucl. Phys. B* **203** (1982) 140–156.
- [78] M. Buballa, *NJL model analysis of quark matter at large density*, *Phys. Rept.* **407** (2005) 205–376, [[hep-ph/0402234](#)].
- [79] A. Dumitru, R. D. Pisarski, and D. Zschiesche, *Dense quarks, and the fermion sign problem, in a SU(N) matrix model*, *Phys. Rev. D* **72** (2005) 065008, [[hep-ph/0505256](#)].
- [80] Y. Bai, T.-K. Chen, and M. Korwar, *QCD-collapsed domain walls: QCD phase transition and gravitational wave spectroscopy*, *JHEP* **12** (2023) 194, [[arXiv:2306.17160](#)].
- [81] A. R. Zhitnitsky, *'Nonbaryonic' dark matter as baryonic color superconductor*, *JCAP* **10** (2003) 010, [[hep-ph/0202161](#)].
- [82] Z. F. Seidov, *The Stability of a Star with a Phase Change in General Relativity Theory*, *Sov. Astron.* **15** (1971) 347–348.
- [83] K. Schertler, C. Greiner, J. Schaffner-Bielich, and M. H. Thoma, *Quark phases in neutron stars and a 'third family' of compact stars as a signature for phase transitions*, *Nucl. Phys. A* **677** (2000) 463–490, [[astro-ph/0001467](#)].
- [84] M. G. Alford, S. Han, and M. Prakash, *Generic conditions for stable hybrid stars*, *Phys. Rev. D* **88** (2013), no. 8 083013, [[arXiv:1302.4732](#)].
- [85] C. Csáki, C. Eröncel, J. Hubisz, G. Rigo, and J. Terning, *Neutron Star Mergers Chirp About Vacuum Energy*, *JHEP* **09** (2018) 087, [[arXiv:1802.04813](#)].
- [86] G. Ventagli, P. G. S. Fernandes, A. Maselli, A. Padilla, and T. P. Sotiriou, *Neutron stars and the cosmological constant problem*, *Phys. Rev. D* **111** (2025), no. 2 024001, [[arXiv:2404.19012](#)].
- [87] S. Weinberg, *The Cosmological Constant Problem*, *Rev. Mod. Phys.* **61** (1989) 1–23.
- [88] J. Polchinski, *The Cosmological Constant and the String Landscape*, in *23rd Solvay*

*Conference in Physics: The Quantum Structure of Space and Time*, pp. 216–236, 3, 2006.  
[hep-th/0603249](#).

- [89] **Planck** Collaboration, N. Aghanim et al., *Planck 2018 results. VI. Cosmological parameters*, *Astron. Astrophys.* **641** (2020) A6, [[arXiv:1807.06209](#)]. [Erratum: *Astron. Astrophys.* 652, C4 (2021)].
- [90] R. D. Pisarski, *Fuzzy Bags and Wilson Lines*, *Prog. Theor. Phys. Suppl.* **168** (2007) 276–284, [[hep-ph/0612191](#)].
- [91] A. Chodos, R. L. Jaffe, K. Johnson, C. B. Thorn, and V. F. Weisskopf, *A New Extended Model of Hadrons*, *Phys. Rev. D* **9** (1974) 3471–3495.
- [92] A. Chodos, R. L. Jaffe, K. Johnson, and C. B. Thorn, *Baryon Structure in the Bag Theory*, *Phys. Rev. D* **10** (1974) 2599.